AMERICAN METEOROLOGICAL SOCIETY

Earth Interactions

EARLY ONLINE RELEASE

This is a preliminary PDF of the author-produced manuscript that has been peer-reviewed and accepted for publication. Since it is being posted so soon after acceptance, it has not yet been copyedited, formatted, or processed by AMS Publications. This preliminary version of the manuscript may be downloaded, distributed, and cited, but please be aware that there will be visual differences and possibly some content differences between this version and the final published version.

The DOI for this manuscript is doi: 10.1175/EI-D-17-0027.1

The final published version of this manuscript will replace the preliminary version at the above DOI once it is available.

If you would like to cite this EOR in a separate work, please use the following full citation:

Hatchett, B., and D. McEvoy, 2017: Exploring the Origins of Snow Droughts in the Northern Sierra Nevada, California. Earth Interact. doi:10.1175/EI-D-17-0027.1, in press.

Exploring the Origins of Snow Droughts in the Northern Sierra Nevada, California

Benjamin J. Hatchett[1,2*] and Daniel J. McEvoy[1,2]

[1]Division of Atmospheric Sciences, Desert Research Institute, Reno, Nevada

[2]Western Regional Climate Center, Desert Research Institute, Reno, Nevada

Revised for *Earth Interactions*

December 15, 2017

*Corresponding Author

Benjamin J. Hatchett

benjamin.hatchett@gmail.com

775-673-7111

Division of Atmospheric Sciences

Desert Research Institute, Reno, Nevada

2215 Raggio Parkway

Reno, Nevada, 89512

Abstract

The concept of snow drought is gaining widespread interest as the climate of snow-dominated mountain watersheds continues to change. Warm snow drought is defined as above or near average accumulated precipitation coinciding with below average snow water equivalent at a point in time. Dry snow drought is defined as below average accumulated precipitation and snow water equivalent at a point in time. We contend that such point-in-time definitions might miss important components of how snow droughts originate, persist, and terminate. Using these simple definitions and a variety of observations at monthly, daily, and hourly timescales, we explore the hydrometeorological origins of potential snow droughts in the northern Sierra Nevada from water years 1951 to 2017. We find that snow droughts can result from extreme early season precipitation, frequent rain on snow events, and low precipitation years. Late season snow droughts can follow persistent warm and dry periods with effects that depend upon elevation. Many snow droughts were characterized by lower snow fractions and frequent midwinter peak runoff events. Our findings can guide improved evaluations of historical and potential future snow droughts, particularly with regards to how impacts on water resources and mountain ecosystems may vary depending on how snow droughts originate and evolve in time.

1. Introduction

Drought conditions and record low snowpacks in the western United States during water years (WY; 1 October-30 September) 2014 and 2015 provided incentive to study the emerging phenomenon known as snow drought (Cooper et al. 2016, Mote et al. 2016). The simplest definition of snow drought is near or above average accumulated precipitation (P) coinciding with below average snow water equivalent (SWE) at a point in time, typically 1 April when the

climatological maximum of SWE occurs (Pederson et al. 2011). Harpold et al. (2017) expanded this definition into two types of snow droughts: warm snow drought, where October through March accumulated P is greater than 100% of normal and SWE is less than 100% of normal on 1 April and dry snow drought, where October through March accumulated P is less than 100% of normal and SWE is less than 100% of normal on 1 April. Beyond simple evaluations (e.g., Sproles et al. 2017) little attention has been given to the temporal evolution of snow droughts in terms of persistent dry spells or individual storm events. Understanding the hydrometeorological processes that create snow droughts will aid in evaluating their impacts on consumptive uses that depend on snowmelt-derived runoff or ecological processes that depend on the presence of a snowpack. At present, these specific impacts are not well characterized beyond broad knowledge that shifts from snow to rain reduce warm season streamflow (Berghuijs et al. 2014) and that warming winters cause less efficient snowmelt (Barnhart et al. 2016).

We postulate that defining snow drought based upon single points in time (i.e., 1 April) may result in misleading evaluations of snow droughts by ignoring the mechanisms that lead to their onset. Our purpose is to show how eight snow drought years identified on 1 April in the northern Sierra Nevada (Fig. 1) can have varying hydrometeorological origins through the use of observational data at monthly, daily, and hourly timescales. The results lead us to recommend that snow droughts identified by the simple definitions given by Harpold et al. (2017) are explored temporally to understand the root cause of the identified P/SWE divergence. We also recommend that continuous observations of snow drought be implemented in order to identify early- and mid-winter snow droughts that were later terminated by subsequent snowfall prior to 1 April. The goals of these recommendations are to improve subsequent studies focused on

examining how snow droughts impact hydrologic, ecologic, and socioeconomic systems as well as identifying future snow drought likelihood in regions dependent on snow-derived water resources.

2. Data and Methods

Monthly snow course data (https://wcc.sc.egov.usda.gov/nwcc/rgrpt?report=snowcourse) from 18 snow courses (Fig. 1) and P estimates from the Parameter Regression Independent Slope Method model (PRISM; Daly et al. 2008) were used to identify warm snow droughts based upon 1 April accumulated P > 100% and SWE < 100% of normal. Dry snow droughts were identified based upon 1 April accumulated P <100% and SWE < 100% of normal. Each snow course had at least 80% of the 1981-2010 climatology period in the record. Monthly values of temperature (T) and P from the PRISM grid point nearest to three snow courses (Fig. 1) spanning low (1997 m), middle (2103 m), and high elevations (2591 m) are included to examine the evolution of these snow droughts as a function of elevation. We define early, middle, and late onset snow droughts based upon the time their onset was identified, with October-November characterizing early, December-February as middle, and late onset as March-April.

To explain the observed accumulated P/SWE ratios and explore impacts on streamflow, we included the following additional observations in our analysis: 1) Daily, quality controlled P, T, and SWE from three SNOwpack TELemetery (SNOTEL) stations (Tahoe City Cross (2072 m), Squaw Valley Gold Coast (2442 m), and Fallen Leaf Lake (1903 m); Fig. 1) acquired from the National Resources Conservation Service (https://www.wcc.nrcs.usda.gov/snow/), 2) brightband-derived snow levels (White et al. 2010) from the NOAA Hydrometeorological

87 Testbed/California Department of Water Resources (DWR)-supported snow level radar located
88 at Colfax, CA, which was acquired from the Earth Systems Research Laboratory
89 (http://www.esrl.noaa.gov), 3) daily streamflow from the North Fork of the American River
90 acquired from the United States Geological Survey
91 (https://waterdata.usgs.gov/nwis/uv?site_no=11427000), 4) GPS-measured precipitable water
92 from the Bodega Bay Atmospheric River Observatory acquired from suominet
93 (http://www.suominet.ucar.edu/; Ware et al. 2000), 5) P values from a DWR weather station at
94 Blue Canyon (1610m; http://cdec.water.ca.gov/), and 6) daily maximum T and accumulated P
95 from five National Weather Service Cooperative Observer (COOP) stations located in the
96 northern Sierra Nevada above 1300 m elevation with 90% complete records from October 1950
97 to February 2017 acquired from the ACIS database (http://scacis.rcc-acis.org/).
98
99 We calculated the fraction of precipitation as snow (hereafter snow fraction) using the Dai
100 (2008) equation, which estimates conditional probabilities of snow as a function of T with
101 parameter values for the Sierra Nevada ecoregion (Rajagopal and Harpold (2016). We calculated
102 the snow fraction for October-March (February in 2017) and took the five-station average over
103 this period.
104
105 **3. Results and Discussion**
106 **3.1 A Historical Monthly Perspective Using Snow Courses**
107 Seven snow drought years are identified from snow course data using the 1 April P/SWE criteria
108 (Fig. 2a). One is a warm snow drought (WY1951), two are influenced by singular wet events
109 (WY1963) or wet periods (WY1997), two are late onset snow droughts (WY1970 and WY2016),

and two are dry snow droughts (WY1977 and WY2015). Figure 3 shows monthly evolutions of these snow droughts via PRISM estimates of T and P and first-of-the-month SWE measurements for three snow courses (bold outlined dots in Fig. 1). WY1951 represents a classic warm snow drought. This year was characterized by late fall (October-November) having well above normal P and anomalously warm conditions followed by a wetter than normal winter (December-January) while late winter (February-March) was dry and cool. WY1963 demonstrates how a singular wet event can obscure an otherwise dry snow drought year, instead leading to its categorization as a warm snow drought. WY1963 began with an extremely wet October resulting from the warm and wet Columbus Day Storm of 1962 and was followed by a dry and anomalously warm winter. The October event created early snow drought conditions with divergent P (above normal) and SWE (below normal). Wetter than normal conditions during February-March provided marginal SWE gains, however the 1 April P/SWE ratio satisfied the snow drought criteria. WY1997 provides another example of how an extremely wet period (the 1997 flood; Lott et al. 1997; Kaplan et al. 2009) can facilitate producing a snow drought year. Average T during WY1997 did not appear to play a major role in producing snow drought conditions, although a dry and warm March reduced SWE at the low elevation snow course (Fig. 3g). This created a late onset snow drought due to above average accumulated P. The high snow levels during the 1997 flood event melted substantial snow (Underwood et al. 2009; Kaplan et al. 2009) and resulted in strong elevation dependence of warm snow drought conditions (Figure 2c). WY1970 and WY2016 (see next section) also appear as late onset snow droughts. The limitation of using a monthly time step becomes evident when trying to assess the precise processes causing WY1970 to transition into snow drought. WY1977 is a classic dry snow drought where P and SWE were both much below normal. WY2015, noted for its exceptional lack of snow

(Belmecheri et al. 2015) and persistent above normal T (Fig. 3), is classified as a dry snow drought due to low P (Fig. 3; Harpold et al. 2017).

3.2 Daily Data Reveals Onset of the 2016 Snow Drought

Daily observations of P and SWE from SNOTEL stations provided information relevant to the late season snow drought onset during WY2016. As previously shown in other water years, the influence of elevation on snow drought appears in snow course data (Fig. 2c). In 2016, the elevation dependence of % of normal 1 April SWE is shown by above normal conditions at the highest elevation station but below normal at the lowest elevation station (cf. Fig. 3c and 3i). Daily data at the Tahoe City Cross station illustrates this further (Fig. 4) as both accumulated P and SWE were near or above median values through February 2016. However, two dry periods with anomalously warm conditions during February (Fig. 3a,d,g and Fig. 4a; right y-axis) coincided with SWE depletion to below median values. This period marked the onset of snow drought at Tahoe City, with accumulated P above and SWE below normal. Although P accumulations continued in March and April, only marginal SWE recovery occurred due to above normal T during March (Fig. 3). Using the normalized difference snow index (NDSI) values from the MODIS mission and acquired using the Google Earth Engine-driven Climate Engine (Huntington et al. 2017), the shift from an above-normal early season snowpack to widespread low-elevation snow drought (cf. Fig 4b and 4c) following the warm, dry period is shown spatially. Remotely sensed products such as NDSI may provide valuable data for real-time snow drought monitoring in conjunction with ground-based station observations.

3.3 A Case Study of 2017

Daily and hourly observations add further insight to the physical processes driving onset and termination phases of snow droughts. During the early portion of WY2017, concern mounted as to whether WY2017 would become a warm snow drought year. Lack of snow during the Christmas-New Year's period can have marked economic impacts on winter tourism in the northern Sierra Nevada. To examine the sequence of events leading to warm snow drought onset and termination between 1 October – 28 February 2017, we use daily P and SWE data from two SNOTEL stations, a higher elevation station at Squaw Valley Gold Coast (2442 m; hereafter Squaw; Fig. 5a) and a lower elevation station at Fallen Leaf (1902 m; Fig. 5b). Hourly observations (Fig. 5c-e) are included to facilitate explanation of the processes driving snow drought variability.

Early WY2017 featured multiple landfalling atmospheric rivers (Fig. 5e; defined following Ralph et al. 2004) producing copious P with very high snow levels (> 2500 m) and little snow accumulation. A dry November marked the onset of snow drought conditions (O1; brown boxes) at Squaw. A higher snow level storm in early December led to recovery at Squaw, but produced snow drought onset (O1F) at Fallen Leaf. A moderate snow level atmospheric river event contributed substantial P with SWE increase at both SNOTEL stations leading to snow drought termination (T1F) on 3-5 January at Fallen Leaf. A higher snow level atmospheric river event during 8-10 January nearly brought Fallen Leaf back into snow drought due to appreciable rain-on-snow. During the remainder of February, SWE at both elevations rose steadily, with one exception being another high snow level and wet atmospheric river on 8-9 February. No further periods of snow drought were observed.

179 WY2017 demonstrated the utility of employing daily and sub-daily observations in terms of
180 monitoring potential snow drought onsets and terminations and their root causes including
181 prolonged dry spells and high snow level precipitation events. Snow level radar data showed
182 how differing phases of P associated with heavy P events caused melting and accumulation of
183 snow to vary with time and by elevation on a storm-by-storm basis. Atmospheric rivers, which
184 provide large P totals and frequent rain-on-snow events due to warmer temperatures and higher
185 snow levels (Guan et al. 2016; Hatchett et al. 2017), appeared to contribute to snow drought
186 onset and termination during WY2017. The correspondence between atmospheric river
187 conditions, heavy P and high snow levels with varying low elevation SWE behavior and
188 streamflow peaks (Fig. 5d) emphasizes how high frequency observations facilitate explanation of
189 the hydrometeorological processes that contribute to snow drought variability. Examination of
190 multiple stations at high frequency intervals can also aid in identifying potentially impactful
191 snow drought conditions, such as low elevation snow drought ("O1F" in Figure 5).
192
193 **3.4 Snow Fraction and Midwinter Streamflow**
194 Partitioning total P into snow fractions and examining midwinter peaks in streamflow gives
195 additional process-based insight into the origins and implications of snow droughts. In six of
196 seven snow droughts, the snow fractions (Fig. 6a) are below the five-year moving average (thick
197 black line on Fig. 6a). Four of the lowest snow fractions observed over the period studied
198 occurred during snow drought years. Four of the seven snow drought years coincided with peak
199 midwinter runoff events in the North Fork of the American River (Fig. 6b). This result is
200 consistent with low snow fractions as rain-on-snow contributes to mid-winter runoff and
201 snowpack losses or minimal gains (Fig. 5). Under future climate regimes (Klos et al. 2014)

where stronger storms are likely (Lavers et al. 2015), the concern of shifting P phase towards more rain (lower snow fractions) in T sensitive mountain ranges such as the Sierra Nevada (Safeeq et al. 2015; Hatchett et al. 2017) implies that snow drought may become increasingly frequent, especially in lower elevation mountains such as the northern Sierra Nevada. The WY2015-2017 period may be an excellent test case for future climate regimes and how managers can adapt to them. During these three years, P covered the full range of hydroclimatic extremes (anomalously low to anomalously high) and three consecutive years of different flavors of snow droughts were observed: dry in WY2015, late onset in WY2016, and early season in WY2017.

4. Concluding Remarks

While not a comprehensive evaluation of all historic snow droughts in the northern Sierra Nevada, our preliminary findings indicate that snow droughts have varied mechanistic origins. The temporal divergence of P to SWE can be used as a metric to estimate the onset of snow drought conditions (Sproles et al. 2017), particularly when examined in conjunction with anomalous T (Cooper et al. 2016, Harpold et al. 2017) and the characteristics of individual storms. These characteristics include snow levels during significant P events, persistence of warm and dry conditions, or singular storm events. Years that do not satisfy the snow drought criteria applied on 1 April (WY2017) should still be evaluated to identify early winter snow drought conditions and potential impacts to ecological processes (e.g., Campbell et al. 2005) and socioeconomic impacts (e.g., Harpold et al. 2017). Warm snow droughts frequently corresponded with water years that included lower fractions of total precipitation falling as snow and often included midwinter flood events, implying that rain-on-snow events often create warm

225 snow drought conditions. We hope that the considerations presented herein will yield robust
226 snow drought climatologies, assist in developing real-time snow drought monitoring that
227 assimilates high-resolution observational data, and in characterizing time-dependent snow
228 drought impacts. The importance of sub-monthly data is highlighted by aiding the identification
229 of specific processes producing (or terminating) snow droughts, such as winter heat waves or
230 extreme precipitation events with high snow levels. It also facilitates understanding of potential
231 impacts, such as midwinter peak streamflow following rain-on-snow events. Future research
232 should focus on identifying relevant timescales (durations and timing of onset) of snow drought
233 impacts for hydrologic and ecological processes. For example, hydrologic modeling could
234 identify threshold responses in watersheds to changes in precipitation phase and snowpack
235 accumulation patterns relevant for water resource management.
236
237 **Acknowledgements**
238 The project described in this publication was supported by Grant Number G14AP00076 from the
239 United States Geological Survey. Its contents are solely the responsibility of the authors and do
240 not necessarily represent the official views of the USGS. This manuscript is submitted for
241 publication with the understanding that the United States Government is authorized to reproduce
242 and distribute reprints for Governmental purposes. We thank N. Oakley, S. Hatchett, and two
243 anonymous reviewers for constructive comments that improved this manuscript.
244
245 **References**
246 Belmecheri, S., F. Babst, E. R. Wahl, D. W. Stahle, and V. Trouet, 2015: Multi-century
247 evaluation of Sierra Nevada snowpack. *Nat*. *Clim*. *Change*, **6**, 2-3, doi:10.1038/nclimate2809.

Campbell, J.L., M.J. Mitchell, P.M. Groffman, L.M. Christenson, and J.P. Hardy, 2005: Winter in northeastern North America, a critical period for ecological processes. *Front. Ecol. Env., 3(6)*, 314-322.

Cooper, M. G., A.W. Nolin, and M. Safeeq, 2016: Testing the recent snow drought as an analog for climate warming sensitivity of Cascades snowpacks. *Environ. Res. Lett.*, **11**, 84009, doi:10.1088/1748-9326/11/8/084009, 2016.

Daly, C., M. Halbleib, J.I. Smith, W.P. Gibson, M.K. Doggett, G.H. Taylor, J. Curtis, and P.A. Pasteris, 2008: Physiographically-sensitive mapping of temperature and precipitation across the conterminous United States. *Int. J. Climatol.* **28**, 2031-2064, doi:10.1002/joc.1688.

Guan, B., D. E. Waliser, F. M. Ralph, E. J. Fetzer, and P. J. Neiman, 2016: Hydrometeorological characteristics of rain-on-snow events associated with atmospheric rivers. *Geophys. Res. Lett.*, **43**, 2964–2973, doi:10.1002/2016GL067978.

Harpold, A. A., M. Dettinger, and S. Rajagopal, 2017: Defining snow drought and why it matters. *Eos*, **98**, doi:10.1029/2017EO068775.

Hatchett, B.J.; B. Daudert, C.B. Garner, N.S. Oakley, A.E. Putnam, and A.B. White, 2017: Winter Snow Level Rise in the Northern Sierra Nevada from 2008 to 2017. *Water*, **9**, 899, doi:10.3390/w9110899.

Huntington, J., K. Hegewisch, B. Daudert, C. Morton, J. Abatzoglou, D. McEvoy, and T. Erickson, 2017: Climate Engine: Cloud Computing and Visualization of Climate and Remote Sensing Data for Advanced Natural Resource Monitoring and Process Understanding. *Bull*. *Amer*. *Meteor*. *Soc*. doi:10.1175/BAMS-D-15- 00324.1, 98:11, 2397-2410, https://doi.org/10.1175/BAMS-D-15-00324.1.

Kaplan, M.L., C.S. Adaniya, P.J. Marzette, K.C. King, S.J. Underwood, and J.M. Lewis, 2009: The Role of Upstream Midtropospheric Circulations in the Sierra Nevada Enabling Leeside (Spillover) Precipitation. Part II: A Secondary Atmospheric River Accompanying a Midlevel Jet. *J*. *Hydrometeor*. **10**, 1327–1354, https://doi.org/10.1175/2009JHM1106.1.

Klos, P. Z., T. E. Link, and J. T. Abatzoglou, 2014: Extent of the rain-snow transition zone in the western U.S. under historic and projected climate, *Geophys*. *Res*. *Lett*. **41**, 4560–4568, doi:10.1002/2014GL060500.

Lavers, D. A., F. M. Ralph, D. E. Waliser, A. Gershunov, and M. D. Dettinger, 2015: Climate change intensification of horizontal water vapor transport in CMIP5, *Geophys*. *Res*. *Lett*. **42**, 5617–5625, doi:10.1002/2015GL064672.

Lott, N., D. Ross, and M. Sittel, 1997: The winter of ’96–’97 West Coast flooding. National Climatic Data Center, Tech. Rep. 97-01, 22 pp.

294 Mote, P. W., D. E. Rupp, S. Li, D. J. Sharp, F. Otto, P. F. Uhe, M. Xiao, D. P. Lettenmaier, H.
295 Cullen, and M. R. Allen, 2016: Perspectives on the causes of exceptionally low 2015 snowpack
296 in the western United States, *Geophys*. *Res*. *Lett*. **43**, 10,980–10,988,
297 doi:10.1002/2016GL069965.
298
299 Pederson, G. T., S. T. Gray, C. A. Woodhouse, J. L. Betancourt, D. B. Fagre, J. S. Littell, E.
300 Watson, B. H. Luckman, and L. J. Graumlich (2011), The unusual nature of recent snowpack
301 declines in the North American cordillera. *Science*, 333, 332-335, doi:10.1126/science.1201570.
302
303 Ralph, F. M., P. J. Neiman, and G. A. Wick, 2004: Satellite and CALJET aircraft observations of
304 atmospheric rivers over the eastern North-Pacific Ocean during the El Niño winter of 1997/98.
305 *Mon*. *Weather Rev*., **132**, 1721–1745.
306
307 Safeeq, M., S. Shukla, I. Arismendi, G.E. Grant, S.L. Lewis, and A. Nolin, 2016, Influence of
308 winter season climate variability on snow–precipitation ratio in the western United States. *Int*. *J*.
309 *Climatol*. **36**, 3175–3190. doi:10.1002/joc.4545.
310
311 Sproles, E. A., T.R. Roth, and A.W. Nolin, 2017: Future snow? A spatial-probabilistic
312 assessment of the extraordinarily low snowpacks of 2014 and 2015 in the Oregon Cascades. *The*
313 *Cryosphere*, **11**, 331-341, doi:10.5194/tc-11-331-2017.
314
315 Underwood, S.J., M.L. Kaplan, and K.C. King, 2009: The Role of Upstream Midtropospheric
316 Circulations in the Sierra Nevada Enabling Leeside (Spillover) Precipitation. Part I: A Synoptic-

Scale Analysis of Spillover Precipitation and Flooding in a Leeside Basin. *J*. *Hydrometeor*. **10**, 1309–1326, https://doi.org/10.1175/2009JHM1105.1.

Ware, R.H. D. W. Fulker, S. A. Stein, D. N. Anderson, S. K. Avery, R. D. Clark, K. Droegemeier, J. P. Kuettner, and J. B. Minster, 2000: Suominet: A real-time national GPS network for atmospheric research and education. *Bull*. *Amer*. *Meteor*. *Soc*., **81**, 677-694.

White, A., D. Gottas, A. Henkel, P. Neiman, F. Ralph, and S. Gutman, 2010: Developing a Performance Measure for Snow-Level Forecasts. *J*. *Hydrometeor*. **11**, 739–753, doi: 10.1175/2009JHM1181.1.

List of Figures

Figure 1: Map of the Northern Sierra Nevada study area. Snow course dots with bold outlines were used in Fig. 3.

Figure 2: (a) Scatterplot of PRISM October-March accumulated P and snow course SWE for 1 April during the period spanning WY1951-2017 as a percentage of 1981-2010 medians. Each dot represents a different snow course. All years are shown in grey with identified snow droughts colored. WY2017 (black dots) is also shown since although it failed to be classified as a snow drought on 1 April, snow drought conditions were present during November-December. WY2017 is presented as a case study in section 3.3. (b) Percentage of 1 April 1981-2010 median snow course SWE versus elevation for WY1970. (c) As in (b) except for WY1997.

Figure 3: Monthly evolution of T (a) P (b), and SWE (c) for seven snow droughts at Carson Pass (elevation 2591 m). (d-f) as in (a-c) but for Donner Pass (elevation 2103 m). (g-i) as in (a-c) but for Camp Richardson (elevation 1997 m). T values are anomalies (in °C) and P and SWE values are percent of 1981-2010 climatology.

Figure 4: (a) Time series of 1981-2010 median and WY2016 observed SWE, P, and T anomalies for the Tahoe City Cross SNOTEL spanning 1 October 2015 to 30 April 2016. MODIS-derived normalized snow difference index values (differenced from 2002-2017 averages) for the 30-day periods during no snow drought (b) and after the onset of low elevation snow drought (c).

Figure 5: (a) Median 1981-2010 precipitation (P; salmon) and snow water equivalent (SWE; light blue) and WY2017 observed P (red) and SWE (dark blue) at Squaw Valley Gold Coast SNOTEL for 1 October – 28 February 2017. (b) As in (a) but for Fallen Leaf SNOTEL. (c) Brightband-derived snow levels derived from the Colfax, CA snow level radar. (d) Streamflow at gauge on the North Fork of the American River. (e) GPS-derived total precipitable water at Bodega Bay (left) and precipitation at Blue Canyon (right). Blue bars denote atmospheric river events.

Figure 6: (a) Fraction of October-March precipitation estimated as snow and averaged over five COOP stations. Black line shows the five-year moving average. Dots are colored by total October-March precipitation and sized proportional to the median number of precipitation days. (b) Daily observations of October-March streamflow at the North Fork of the American River. The dashed blue line shows the top 0.02% of streamflow from the period 1950-2017. Red boxes on both plots show identified snow drought years (cf. Fig. 2) and the black box shows WY2017.

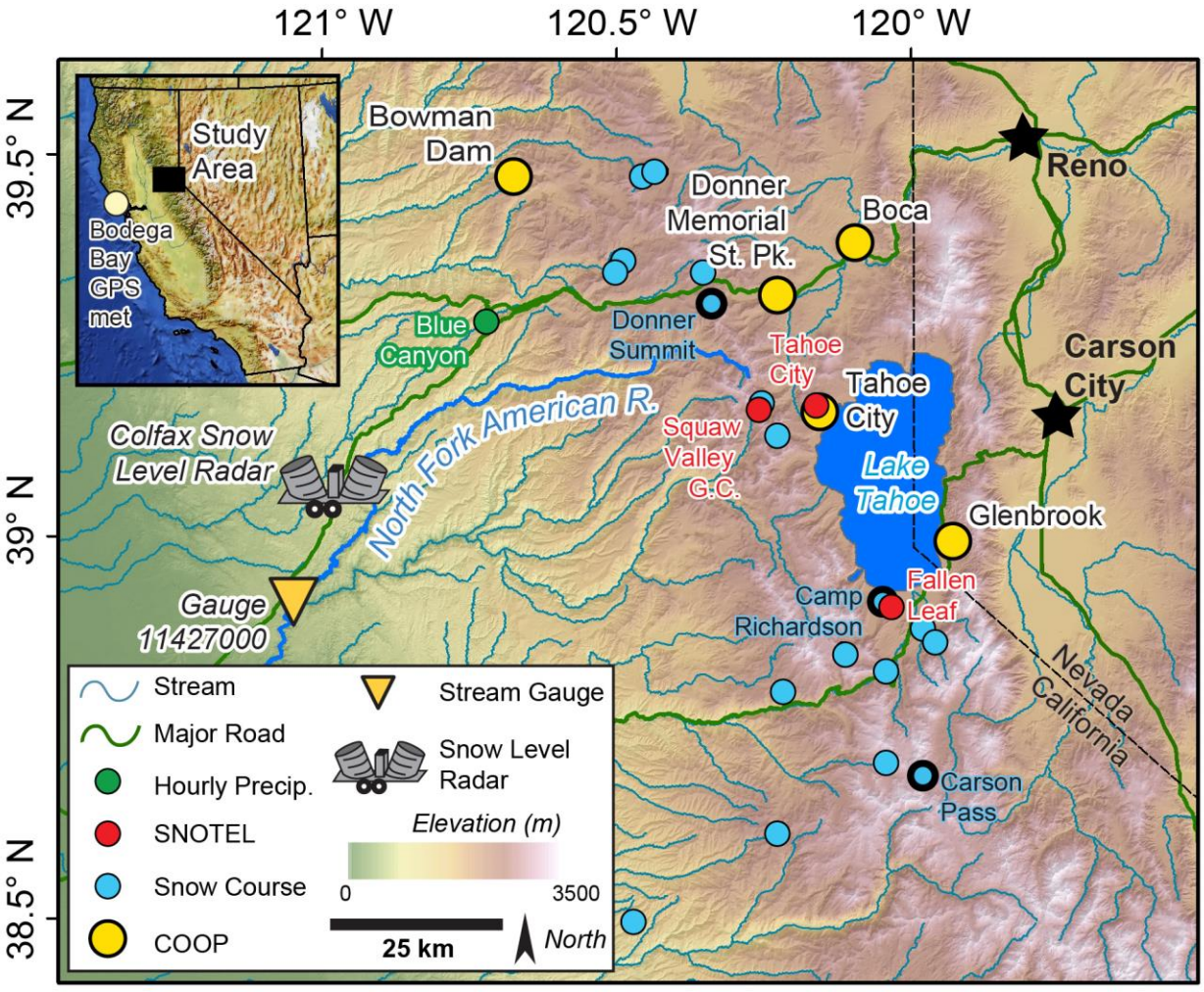

Figure 1: Map of the Northern Sierra Nevada study area. Snow course dots with bold outlines were used in Fig. 3.

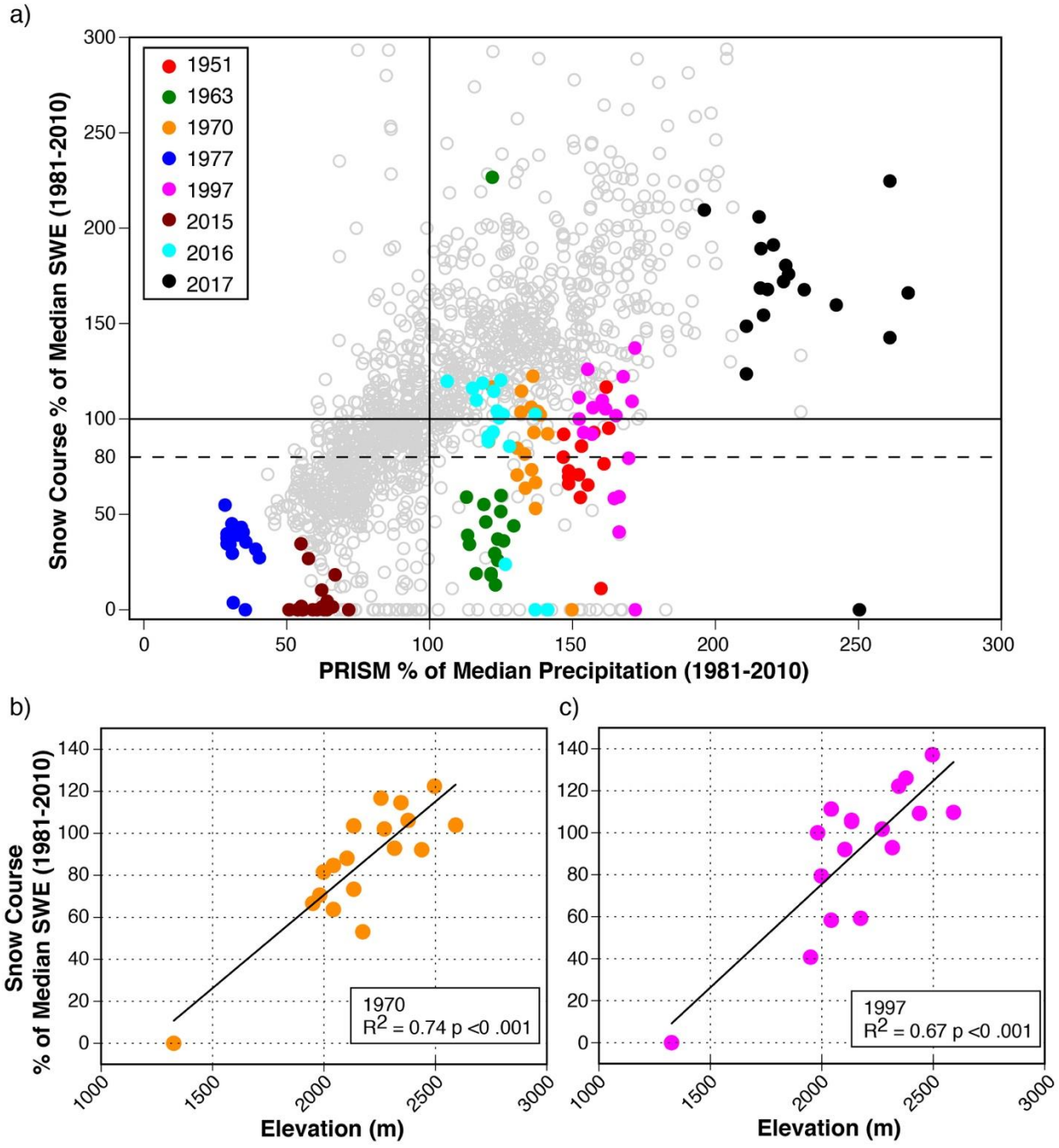

Figure 2: (a) Scatterplot of PRISM October-March accumulated P and snow course SWE for 1 April during the period spanning WY1951-2017 as a percentage of 1981-2010 median values. Each dot represents a different snow course and year. All years are shown in grey with identified snow droughts colored. WY2017 (black dots) is also shown since although it failed to be

373 classified as a snow drought on 1 April, snow drought conditions were present during
374 November-December. WY2017 is presented as a case study in section 3.3. (b) Percentage of 1
375 April 1981-2010 median snow course SWE versus elevation for WY1970. (c) As in (b) except
376 for WY1997.
377

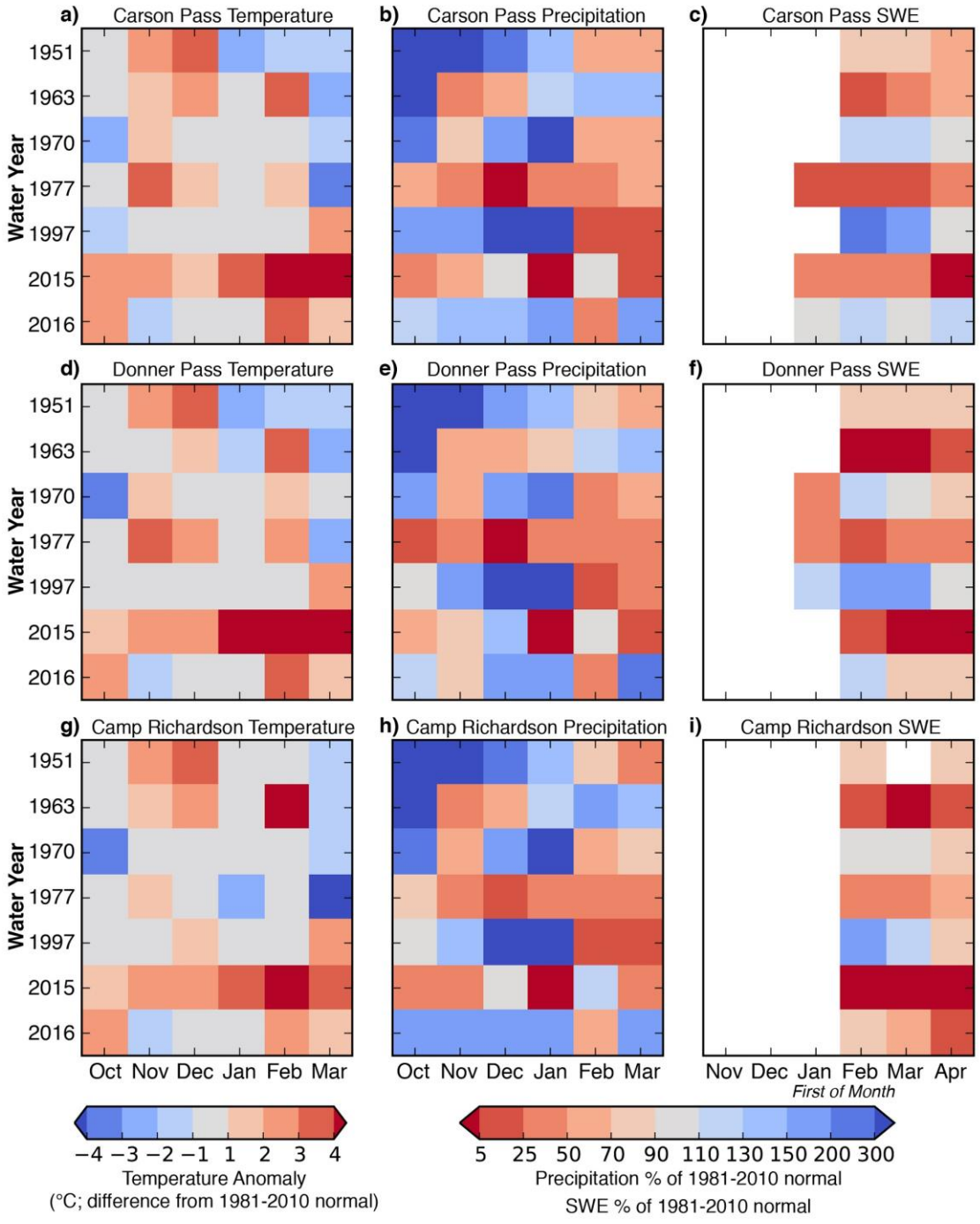

Figure 3: Monthly evolution of T (a) P (b), and SWE (c) for seven snow droughts at Carson Pass (elevation 2591 m). (d-f) as in (a-c) but for Donner Pass (elevation 2103 m). (g-i) as in (a-c) but for Camp Richardson (elevation 1997 m). T values are anomalies (in °C) and P and SWE values are percent of 1981-2010 climatology.

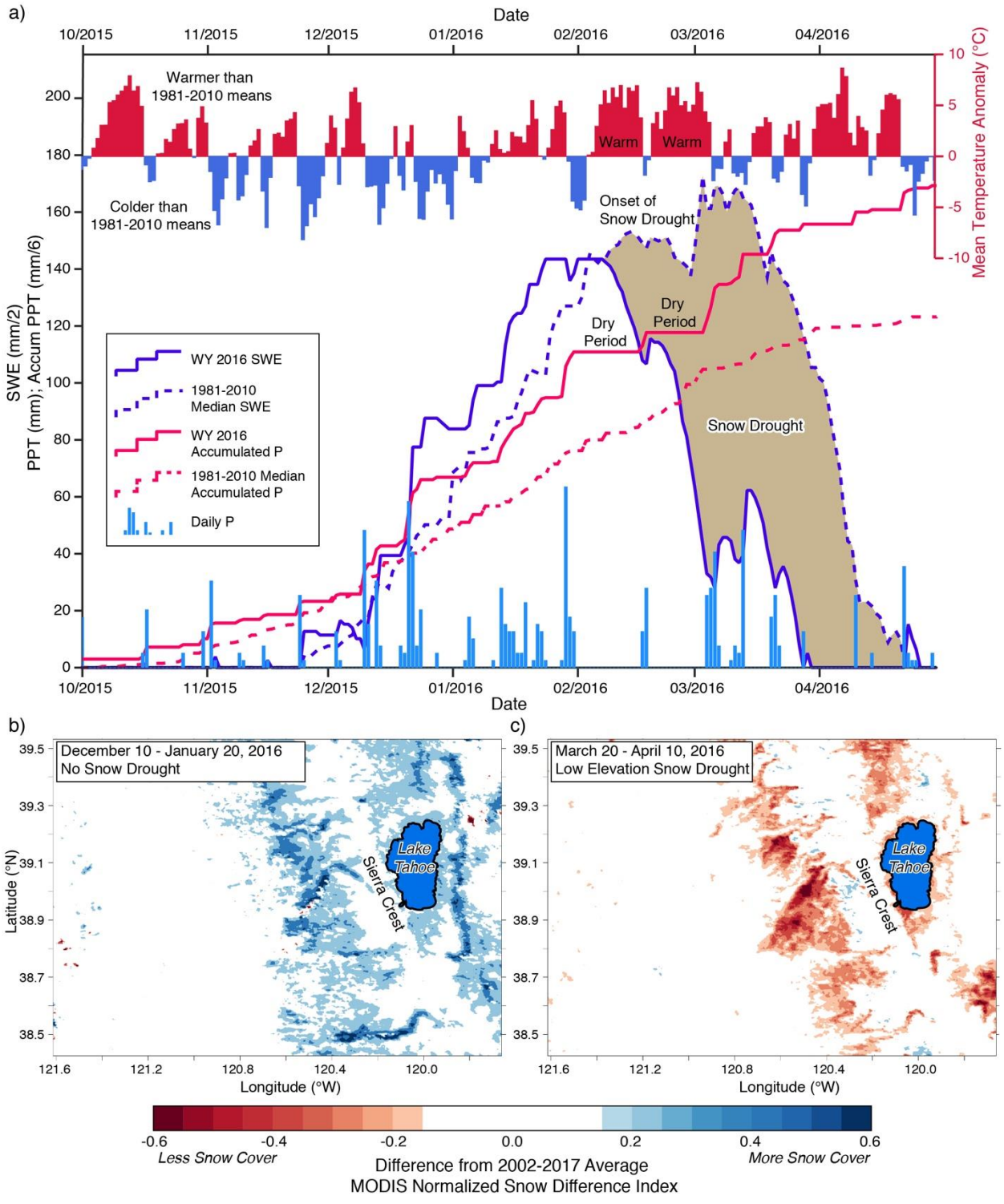

383

384 Figure 4: (a) Time series of 1981-2010 median and WY2016 observed SWE, P, and T anomalies

385 for the Tahoe City Cross SNOTEL spanning 1 October 2015 to 30 April 2016. MODIS-derived

386 normalized snow difference index values (differenced from 2002-2017 averages) for the 30-day
387 periods during no snow drought (b) and after the onset of low elevation snow drought (c).
388

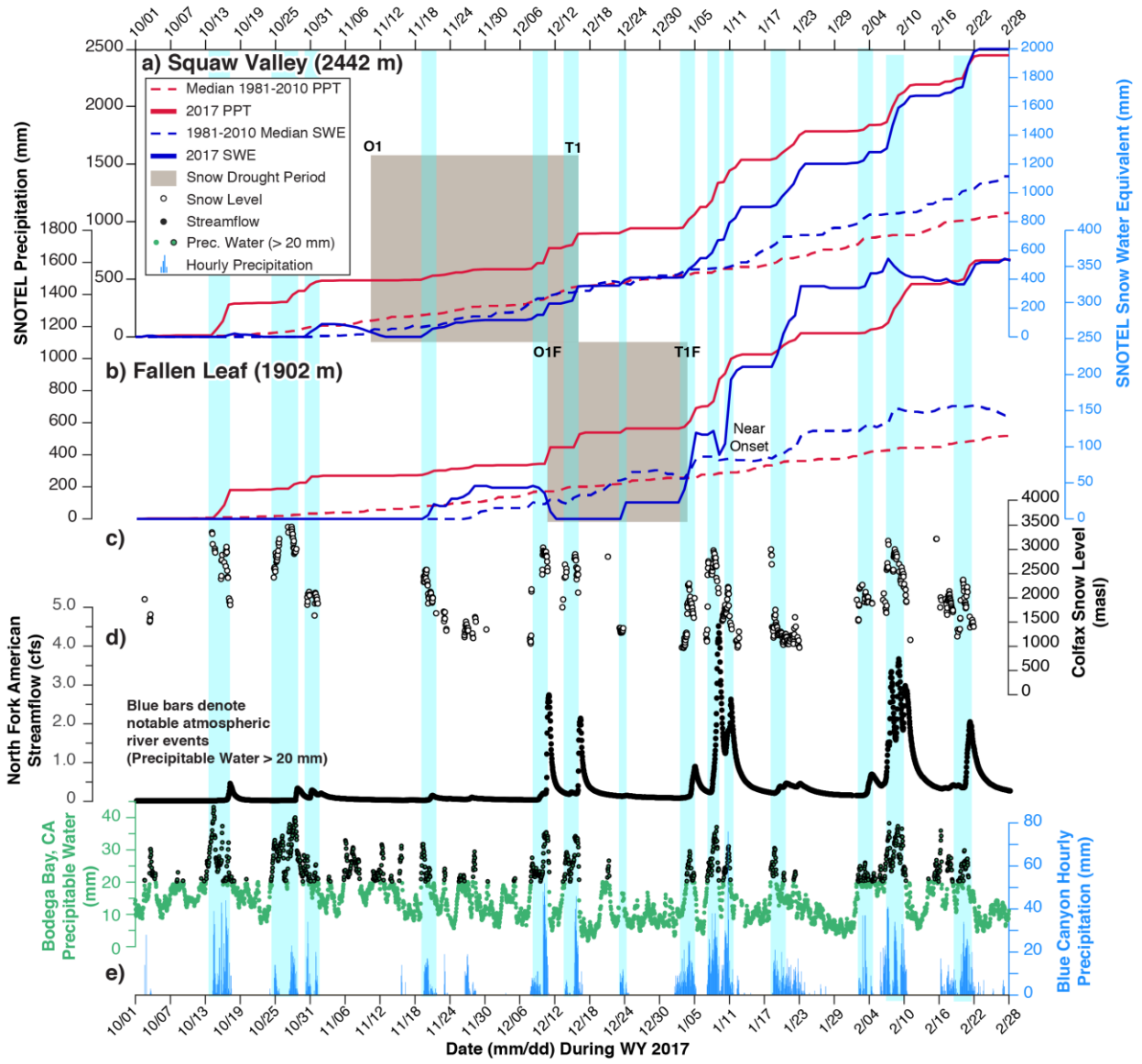

Figure 5: (a) Median 1981-2010 precipitation (P; salmon) and snow water equivalent (SWE; light blue) and WY2017 observed P (red) and SWE (dark blue) at Squaw Valley Gold Coast SNOTEL for 1 October – 28 February 2017. (b) As in (a) but for Fallen Leaf SNOTEL. (c) Brightband-derived snow levels derived from the Colfax, CA snow level radar. (d) Streamflow at gauge on the North Fork of the American River. (e) GPS-derived total precipitable water at Bodega Bay (left) and precipitation at Blue Canyon (right). Blue bars denote atmospheric river events.

397

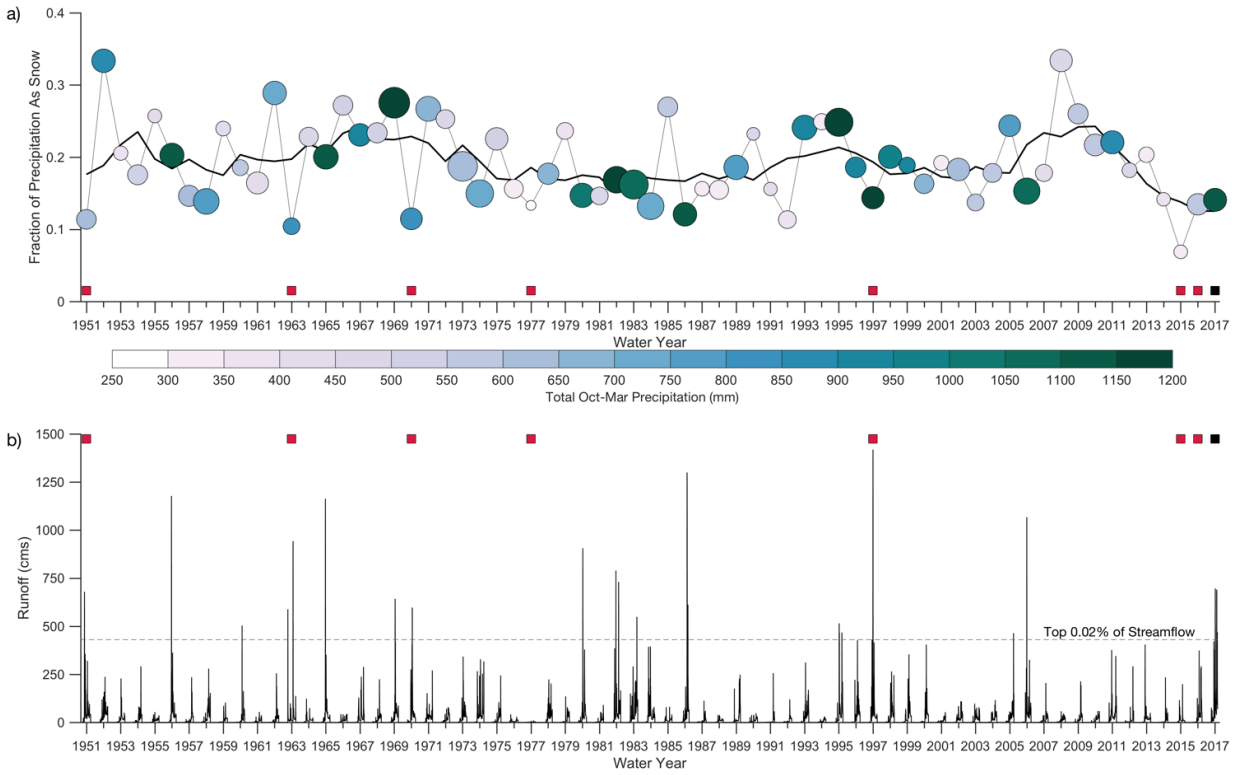

Figure 6: (a) Fraction of October-March precipitation estimated as snow and averaged over five COOP stations. Black line shows the five-year moving average. Dots are colored by total October-March precipitation and sized proportional to the median number of precipitation days. (b) Daily observations of October-March streamflow at the North Fork of the American River. The dashed blue line shows the top 0.02% of streamflow from the period 1950-2017. Red boxes on both plots show identified snow drought years (cf. Fig. 2) and the black box shows WY2017.